Sustainable Energy, Grids and Networks 47 (2026) 102397

Contents lists available at ScienceDirect

Sustainable Energy, Grids and Networks

journal homepage: www.elsevier.com/locate/segan

Assessing the impact of electric vehicles on power grids using sparse mobility data: A GIS- and machine learning-based approach

Davide Fratelli*, Corrado Maria Caminiti, Matteo Spiller, Aleksandar Dimovski, Marco Merlo

Department of Energy, Politecnico di Milano, 20156 Milano, Italy

HIGHLIGHTS

- Probabilistic-based enhancement of the spatial and temporal resolution of trips.
- Machine Learning-based identification of electric vehicle trips.
- Charging profiles aggregated at the Medium Voltage level.
- Grid impact simulation on a real Medium Voltage distribution network.

ARTICLE INFO

Keywords:
Electric Vehicles
Spatial-Temporal Modeling
Grid planning
Geographic Information Systems
Machine learning
Quasi-dynamic simulation

ABSTRACT

The electrification of light-duty transport introduces new and variable demand patterns, challenging distribution network planning and operation. As Electric Vehicle (EV) adoption grows, grid operators need better tools to address this novel demand and formulate decisions on investments and infrastructure upgrades. Yet, limited and low-quality mobility data complicates efforts to assess EV-induced grid stress. This study presents a novel bottom-up spatiotemporal energy model that uses low-resolution mobility data to evaluate electric mobility's impact on distribution networks. By integrating Geographic Information Systems (GIS) and machine learning (ML), the model refines EV selection routines based on journey and driver features. It maps mobility patterns onto real power system elements, using tailored metrics to assess network stress. Using real-world data and implemented on the network twin of a Regional Distribution System Operator (DSO) in northern Italy, the model provides a dataset of geo-referenced EV arrivals with a one-hour resolution, comparing twelve future 2030 scenarios with the current one. The approach offers clear, actionable insights for grid operators and urban planners, bridging the gap between energy and transport infrastructure. The study finds that in the future scenarios, a significant impact is limited geographically to some areas of the Region's capital city and less than 1% of grid elements report values over the operational levels in the most cumbersome scenario. Moreover, this e-mobility-induced stress is confined to the peak traffic hours of the day.

1. Introduction

A significant policy shift to reduce human environmental impact and achieve net-zero goals [1] has emerged in recent years, driven by governmental and institutional efforts. Central to this transition is the widespread electrification of both domestic and industrial energy consumption. In the residential sector, this shift primarily involves the adoption of electric appliances, most notably heat pumps, and the electrification of light-duty vehicles. While partially endogenous, these changes are primarily supported by substantial public subsidies aimed at accelerating consumer adoption. Examples include financial incentives for the purchase of Electric Vehicles (EVs) and investments in charging infrastructure [2,3]. At the European level, the Fit for 55 (FF55) legislative package exemplifies this top-down effort, as it comprises a set of coordinated reforms designed to align EU policies with its climate targets, as endorsed by the European Council and Parliament [4]. Each Member State subsequently transposed these objectives into National Energy and Climate Plans.

* Corresponding author.
Email addresses: davide.fratelli@polimi.it (D. Fratelli), corradomaria.caminiti@polimi.it (C.M. Caminiti), matteo.spiller@polimi.it (M. Spiller), aleksandar.dimovski@polimi.it (A. Dimovski), marco.merlo@polimi.it (M. Merlo).

https://doi.org/10.1016/j.segan.2026.102397
Received 27 February 2026; Received in revised form 26 June 2026; Accepted 27 June 2026
Available online 29 June 2026

Abbreviations

BEV	Battery Electric Vehicles
CP	Charging point
CDF	Cumulative Distribution Function
DN	Distribution network
EU	European Union
EV	Electric Vehicle
EVT	Electric Vehicle Trip
FF55	Fit for 55
GIS	Geographic Information System
ICE	Internal Combustion Engine
MV	Medium Voltage
ML	Machine Learning
MC	Monte Carlo
NHTS	National Household Travel Survey
OD	Origin-Destination
OSM	OpenStreetMaps
QDS	Quasi-Dynamic Simulation

This electrification trend is increasingly evident. Globally, sales of electric cars continued to expand in 2024, accounting for over 20% of the car market. Moreover, worldwide sales of ICE cars decreased by 1.5% in 2024. Pure battery EV sales (BEV) reached over 10 million in 2024, up fivefold since 2020 [5]. As electrification accelerates, it introduces new challenges related to the temporal and spatial variability of electricity demand [6]. Addressing these complexities requires tools capable of guiding strategic investments in grid reinforcement and infrastructure deployment [7].

From a planning perspective, replicating the behaviour of electric fleets in both space and time has become a priority. To this end, spatiotemporal modelling has emerged as a key approach, as it integrates real-world data within GIS to assess the impacts of electric mobility [8–10]. In this context, agent-based traffic simulations are particularly valuable, offering granular insights by simulating synthetic populations with detailed driving behaviours. Yi et al. [10] adopt an open-source framework to model daily traffic patterns based on synthetic agents derived from population samples and socio-demographic data. Each agent is assigned a daily driving profile, enabling the simulation of traffic dynamics and energy use at a regional scale. A similar framework is adopted by Novosel et al. [11] for national-scale EV impact assessments. However, modelling vehicle flows represents only one element of the broader challenge of assessing EV impacts on the power grid. A comparative, non-exhaustive overview of existing modelling approaches and their key features is provided in Table 1.

Tracking of mobility needs and traffic flows is usually performed by leveraging Origin-Destination (OD) matrices [19]. Although quite informative, this modelling approach is not sufficient to achieve the intended objective. Additional factors, such as mode choice and EV adoption rates, must be considered. These are often estimated through tailored surveys: Langbroek et al. [20] compare the travel behaviour of EV users and conventional car users in Sweden, focusing on trip frequency and the share of car travel in overall distance. Their results show that EV users undertake significantly more trips than non-EV drivers. In a similar approach, Danielis et al. [21] analyse data from a 2018 stated-preference survey to investigate the increasing confidence of younger Italian drivers in EV driving range, arguing that future adoption will be driven more strongly by policy incentives than by technological improvements. They also find that EV trips tend to be shorter than those made with conventional vehicles. Another line of research addresses the same issue using machine Learning (ML) models trained on public data sources. For instance, Jia et al. [22] examine EV owner characteristics using the 2017 National Household Travel Survey (NHTS) [23], which offers detailed information on drivers and their trips. They propose a comprehensive EV adoption model that integrates vehicle, personal, and household attributes, and compare several ML algorithms to forecast regional EV penetration across the United States. Likewise, Javid and Nejat [24] develop a multiple logistic regression model using data from the 2012 California Household Travel Survey, later validating it with survey data from the Delaware Valley region.

A common limitation in this body of work, particularly for the purpose of estimating which trips are likely to be made with an EV in traffic models, is the insufficient representation of trip-specific characteristics within adoption frameworks. Miconi et al. [25] address this gap by testing four ML models trained on both regional and provincial public datasets, supplemented with a customised 2019 survey of 300 respondents. Their study highlights the variables most strongly associated with EV adoption. In addition, Li et al. [26] carry out a systematic literature review to identify determinants of consumer intention to adopt battery EVs, proposing key variables for constructing effective adoption models.

On the grid side, assessing the impact of rising EV demand remains a central concern for grid operators. From an energy adequacy perspective, EVs in Europe are expected to consume around 550 TWh by 2030 [27]. Although this figure is substantial, it is not anticipated to pose major challenges in terms of overall energy supply. Instead, the most pressing issues are expected to arise in grid operation and long-term planning. Even though the potential of EVs as distributed storage resources and controllable loads is widely recognised [9], the interaction between network topology and the increasing deployment of fast and ultra-fast chargers introduces significant complexities. Comprehensive impact assessment studies are required to estimate the magnitude and the temporal characteristics of the incremental demand. In this regard, Eitel and Stolle [28] adopt an ML approach to predict the distribution of private charging stations and estimate their effect on the grid.

Table 1
Comparison of EV-traffic-grid studies: models in rows, features in columns.

Model	Grid representation	EV scenario	Demand profile	Traffic model	Data source	Temp. res.	Output metrics
[10]	None	Socio-demographic EV adoption	MC + uncoordinated charging	Agent-based (MATSim) [12]	Socioeconomic data + OD matrix	1 h	Public charging demand
[13]	UK generic distribution grid	Fixed penetration	Monte Carlo (MC) + uncoordinated charging	TransCAD [14]	Origin-Destination (OD) matrix	1 h	Overvoltage, overload
[15]	None	Fleet transition (ICE to EV)	Aggregated energy demand	Dynamic traffic flow model	OD matrix	3 s	Emissions, system energy demand
[16]	Small island LV grid (Azores)	Fixed penetration	MC + uncoordinated charging	Non-Markovian discrete-time process	Travel survey	30 min	Overvoltage, overload
[17]	None	Urban EV uptake	Estimated charging energy	No traffic simulated	20k individual charging stations	1 h	Public charging demand
[18]	None	Fixed penetration	MC + dumb/smart charging	Optimal routing algorithm	OD matrix	5 min	Substation loading

Veldman et al. [29,30] incorporate electricity prices, household loads, and driving patterns into optimisation models that minimise charging costs and peak demand. Salah et al. [31] and Mu et al. [13] investigate the consequences of different charging strategies, smart versus uncoordinated, using scenario-based modelling of EV demand in Switzerland. Gupta et al. [32] conduct a national-level analysis of EV and heat pump penetration, estimating the impact on grid infrastructure and reinforcement costs. These studies use normalised EV load profiles scaled by regional EV counts, emphasising defining charging strategies from a control perspective. While focused on the electric domain, they are conducted at a systemic level and do not consider highly granular spatial or topology-oriented information.

To address the need for greater spatial detail, several high-resolution grid studies have emerged: Vopava et al. [33] advance the state of high-resolution grid representation by adopting a cellular modelling framework that integrates traffic data with 15-minute consumption profiles from German public datasets. While the approach offers detailed geo-referencing, it ultimately relies on a simplified synthetic distribution network (DN) model. In contrast, real DN data are used in [34], where the impact of plug-in buses on Low Voltage (LV) infrastructure is assessed. The study computes the incremental load of 12 buses on an LV feeder with high temporal granularity and uses real demand traces, though it lacks equivalent spatial resolution. Complementary research also explores the coupling of mobility and power systems. The authors of [35] introduce a hierarchical optimisation framework that jointly determines routing decisions and evaluates how electrified long-haul freight transport influences local marginal electricity prices. Their methodology is demonstrated on benchmark systems, including the 24-node Sioux Falls transportation network and the 5-bus PJM grid. Similarly, [36] examines the spatiotemporal evolution of EV charging demand across a 77-node urban road network in China, taking into account travel speeds, distances, congestion, and temperature. Building on comparable principles, the study in [37] couples a 30-node transportation network with a 33-bus DN to estimate charging requirements under various EV penetration scenarios, employing a bidirectional mobility graph and shortest-path routing to model trip flows. Despite substantial methodological contributions, none of these studies simultaneously leverage real-world large-scale mobility data and real-world large-scale distribution-grid data. Moreover, although many adopt bottom-up modelling strategies, they generally focus on small or urbanised areas rather than capturing mobility and grid interactions at broader regional scales.

As a result of the identified gaps above and bearing in mind the comparison in Table 1, this paper contributes to the existing body of research by integrating three key elements: (i) a geo-referenced traffic model derived from a sparse OD matrix, (ii) an ML framework for EV trip (EVT) selection, and (iii) a comprehensive assessment of e-mobility impacts on a real-world DN. Unlike previous studies that focus on generic EV penetration levels [13,28,30,31,33], this work evaluates twelve future scenarios defined by projected adoption rates of both electric vehicles and charging points (CPs). Building on these considerations, the paper addresses two core research questions: i) how can georeferenced mobility demand estimation be coupled with real-world grid impact assessment in a large-scale scenario? Specifically, the aim is to develop a methodology and metrics that link mobility behaviours with their consequences on distribution-grid performance; ii) how can meaningful mobility analyses be conducted when only sparse, aggregated mobility data are available? Given that mobility datasets increasingly serve multiple purposes and cannot always be tailored to specific modelling needs, we investigate strategies to extract robust insights despite these limitations.

The remainder of this paper is organised into four sections. Section 2 details the procedures developed, spanning from the traffic model and EV selection to the design of the charging profiles and lastly the metrics and methods defined to evaluate the impact on the grid. The selected regional case study is outlined in Section 3, along with the specific input data and the comparison of formulated scenarios. Section 4 presents the results, while Section 5 discusses current limitations and the potential extensions of future work.

Table 2
Methodological comparison of the two modelling approaches.

Metric	Existing model [9,18,38]	Present work
Temporal and spatial resolution of the traffic model	The traffic model relies on 24 (hourly) timesteps derived from refined input datasets that have already undergone modelling and validation.	The traffic model is built from a more aggregated dataset containing only three departure time zones. Two methodological contributions are introduced: i) a temporal gravity model for morning departures; ii) a procedure to construct a synthetic dataset for return trips.
Electrical infrastructure detail	Grid characterisation is performed at the primary substation level, considering only the associated service area.	Grid characterisation is carried out at a higher spatial resolution: secondary substations and their service areas are included, and the distribution grid topology (including feeders) is explicitly modelled to quantify impacts.

2. Materials and methods

This study proposes an integrated framework to locate EV charging events and estimate their impact on the DN, extending the existing framework introduced in [9,18,38] along the specific dimensions outlined in Table 2. The methodology, built on sparse mobility data, consists of four steps: (i) a bottom-up traffic model simulates vehicle flows using geospatial and open traffic data; (ii) an ML technique selects EVTs among the simulated journeys; (iii) EVTs are converted into charging profiles; and (iv) the impact on the DN is evaluated based on several metrics, such as voltage levels and grid element loading. EV arrivals are mapped to census sections and aggregated at the level of MV/LV Secondary Substations (SSs). For each SS, an hourly load profile for a representative working day is generated and used as an MV load input in a one-day Quasi-Dynamic Simulation (QDS) in the DIgSILENT PowerFactory model of the real DN. The overall integrated procedure is depicted in Fig. 1, where the input datasets are highlighted in red, and the resulting outputs are shown in green.

2.1. Traffic model principles

The present section describes the extended traffic-model procedure, which builds upon and expands the capabilities developed in [9,18,38]. For both methodologies, the core input consists of a dataset of recorded trips that captures the mobility patterns of a given region, introduced earlier as the sparse matrix. The native characteristics of the available datasets shape the modelling capabilities required in each case. The methodology is organised in two main steps: i) increasing the spatial granularity of trip origins and destinations; ii) improving the temporal characterisation of trips.

The first step relies on a bottom-up, GIS-based approach to analyse and enhance mobility patterns. This begins at the level of census sections, which are defined by the Italian Statistics agency as the most granular homogeneous territorial partition [39]. This dataset is enriched with socioeconomic information and further refines spatial granularity through a geostatistical gravity model. The refinement pivots on probability density functions that incorporate local attributes influencing the likelihood of a given area generating or attracting trips. Different types of trips, namely commuting, education-related travel, leisure, or return-home journeys, dynamically adjust these probabilities. The spatial gravity model enhances spatial resolution by translating municipal

Fig. 1. Information flow and procedures.

origin and destination information into sub-municipal estimates of origin and destination locations. A comprehensive description of the model, including methodological assumptions, is provided in [18].

As a result of this first step, each processed trip is enriched with more granular geographic coordinates of its origin and destination. As introduced in Table 2, one of the objectives of the present work is to generalise the methodology from a region-specific dataset [40] to a more aggregated national survey [41]. In the generalised formulation developed here, the departure time of each trip belongs to one of three coarse temporal categories in the set $F = \{f_1, f_2, f_3\}$. Each category f is associated with a corresponding time interval $[a_x, b_x]$, where a_x and b_x denote, respectively, the lower and upper bounds of the interval for class f_x. To enhance temporal granularity, a uniform distribution is applied within each temporal interval, assigning each bin an equal probability corresponding to the desired time resolution. Specifically, trips belonging to the same temporal class receive a departure time drawn uniformly from the interval $[a_x, b_x]$, as expressed in Eq. (1):

$$t_{\text{dep, travel}} \sim \mathcal{U}(a_x, b_x), \tag{1}$$

where $t_{\text{dep, travel}}$ is the assigned departure time and $\mathcal{U}(a_x, b_x)$ denotes the continuous uniform distribution over the interval $[a_x, b_x]$. This approach redistributes trips uniformly within each temporal band, thereby increasing the model's temporal resolution while remaining consistent with the aggregated structure of the input dataset.

The same approach based on uniform probability distribution is employed when dealing with travel duration d_{travel}. Analogously, this is provided in two classes, the set $D = \{d_1, d_2\}$, each with upper and lower bounds $[a_d, b_d]$. The arrival time is therefore obtained by means of Eq. (2).

$$t_{\text{arr,travel}} = t_{\text{dep,travel}} + d_{travel} \tag{2}$$

A final step to address the correct modelling of return-home trips is required due to the nature of the Italian OD data [41]. Since it is not directly designed to provide an accurate estimate of mobility impact, the information it contains is unidirectional: in simpler terms, it monitors the behaviour and modes of transportation of the population as they travel to their main daily destinations. To estimate return-home mobility, a stay time st_{travel}, defined as a function of the reason for travel μ_r (Eq. (3)), was assigned to each original morning trip, and a synthetic return travel database was generated by inverting departure and arrival points and considering the departure time according to the formulation reported in Eq. (4).

$$st_{travel} \sim \mathcal{N}(\mu_r, \sigma) \tag{3}$$

$$t_{\text{dep,return travel}} = t_{\text{dep,departure travel}} + d_{travel} + st_{travel} \tag{4}$$

A schematic representation of the original dataset structure and the different steps presented in the present section is proposed in Table 3.

2.2. Machine learning vehicle selection model

The following procedure develops an ML model to estimate the likelihood of a trip being an EVT. The model uses publicly available features that are both relevant and correlated with EV adoption. Among private car trips, the algorithm identifies those most likely to be EVTs based on trip features and drivers' socioeconomic characteristics, ranks them by likelihood, and labels trips as electric according to local EV penetration constraints. The procedure can be structured into three main steps: (i) trip characterisation, (ii) model creation and training, and (iii) EVT likelihood estimation and assignment. A detailed schematic of the intermediate steps is shown in Fig. 2.

To apply the ML model, trips mapped from the enhanced OD matrix (Table 3) must first be properly characterised. Each relevant feature at the census section level generates a probability distribution function (PDF). Each trip is then assigned a specific coded classification based on its departure section using random sampling from these distributions. All features are mapped to align with the coding scheme of the learning dataset, ensuring consistency between the target and learning datasets. At this stage, trips are fully characterised with both trip attributes (distance, duration, departure time, purpose) and drivers' socio-economic features. Two separate Random Forest models, one for outward trips and one for return trips, are then applied, yielding a likelihood score for each trip being an EVT.

The Netherlands Mobility Panel (MPN) [42,43] dataset of 2019 is adopted for model training, testing and validation. This annual survey comprises thematic questionnaires at both the person and household levels, linked by unique IDs, allowing each trip to be associated with the corresponding demographic characteristics. Considering feature relevance, independence, and availability in both the learning and target datasets, the final set of variables used to characterise trips is summarised in Table 4.

Finally, once the ML procedure has assigned likelihood scores, indicating how probable each trip is as an EVT, a geographically constrained

Table 3
Example of the original OD matrix (white), the impact of the spatial gravity model (gray), the effect of the temporal gravity model (blue), and the creation of synthetic return trips (Orange).

Orig. Zone	Dest. Zone	Dep. Class	Reason	Orig. Point	Dest. Point	Dep. Time	Duration
Milan 12	Milan 4	f2	Work/Study	$\text{Lat}_{o,1}$ $\text{Long}_{o,1}$	$\text{Lat}_{d,1}$ $\text{Long}_{d,1}$	$t_{\text{dep},1}$	d_1
Milan 14	Milan 1	f3	Leisure	$\text{Lat}_{o,2}$ $\text{Long}_{o,2}$	$\text{Lat}_{d,2}$ $\text{Long}_{d,2}$	$t_{\text{dep},2}$	d_2
Milan 4	Milan 12	-	Ret. Home	$\text{Lat}_{d,1}$ $\text{Long}_{d,1}$	$\text{Lat}_{o,1}$ $\text{Long}_{o,1}$	$t_{\text{dep},1} + d_1 + st_1$	d_1
Milan 1	Milan 14	-	Ret. Home	$\text{Lat}_{d,2}$ $\text{Long}_{d,2}$	$\text{Lat}_{o,2}$ $\text{Long}_{o,2}$	$t_{\text{dep},2} + d_2 + st_2$	d_2

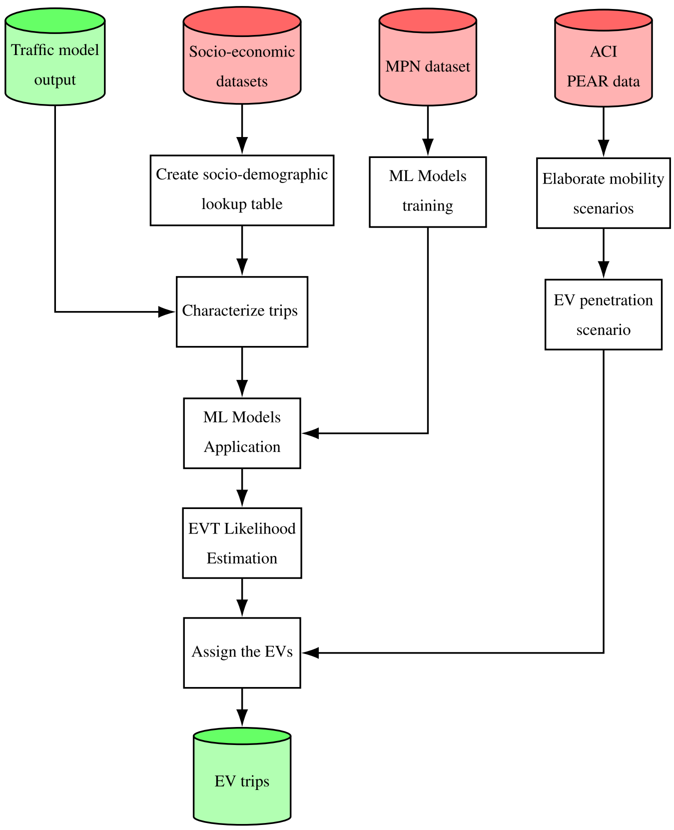

Fig. 2. Flowchart of the ML-based EV choice procedure.

Table 4
Trip and socio-economic features used for ML-based EV selection.

Trip characteristics	purpose, distance, duration, mode, departure time, day of the week
Socio-economic features	gender, employment status, education, age, household income

selection is applied according to the assumed scenario. This constraint is defined at the departure municipality level. In each city, the pool of candidate EVTs is limited to the estimated number of EVs available locally. Trips with the highest likelihood are designated as EVTs only if unassigned EVs are still available in the municipality. A comprehensive description of the model, including validation procedures and parameter tuning, is available in [38].

2.3. Assessing the impact

At the end of the second procedure, a comprehensive dataset tracks temporally and geographically locates the EVTs in the region. To further develop the investigation and address the impact on the electric grid, it is necessary to implement a routine to transition from the geo-referenced vehicular framework to the electrical one, correlating the arrivals in the census sections to arrivals at the most likely SS, which would likely host the recharging demand. First, matrices tracking EVT arrivals and their permanence in census sections are populated, providing an accessible data structure. The transition to the electrical infrastructure is performed, with simplifying assumptions, based on a distance rationale, presented later. Lastly, once the EVTs arrivals and permanence are located on the closest SSs, an algorithm builds the power absorption profiles of each element according to the elaborated scenarios. This last framework is employed in the assessment of the impact with both qualitative and quantitative approaches. As a simplifying assumption, the recharging type is modelled based on the trip purpose. *Return home* trips recharge at private charging stations upon arrival home, while all other trips recharge at public infrastructure.

2.3.1. Traffic matrices

The 15-minute traffic output computed in Section 2.1 is resampled on an hourly basis and elaborated further by building an arrival matrix, a structure that tracks the number of vehicles arriving at each census section over time frames. Moreover, the analysis is enhanced with a *permanence* matrix, which is populated with the number of vehicles parked during each section in a given time frame. An example of the structure is reported in Table 5.

Given the lack of definition of the information related to the distance travelled by each user (as introduced previously, travelling times are very broadly defined), a direct computation of the energy consumed and thus recharged is quite unreliable. To replace an energy information qualitatively, the metric *vehicle-hour* [44] is computed and accumulated in a matrix similar to those introduced above. This metric evaluates the number of vehicles and their stay time, and, in this instance, decreases as the vehicle remains parked and time goes by, reaching zero as it leaves the section. For each time frame τ and section s, considering the j-th vehicle, its departure time dt_j in the set of arrivals in J_s^τ, it is accumulated as shown in Eq. (5):

$$veh_s^\tau = \sum_{j\in J_s^\tau} (dt_j - \tau) \tag{5}$$

2.3.2. Geographical matching of arrivals

As discussed earlier, EVT arrivals are assigned to SSs based on a proximity criterion. This assumption is adopted for both privately charged trips and trips using public charging infrastructure. For private charging, the household at the trip destination is, with few and difficult-to-model exceptions, assumed to be supplied by the nearest SS. Public CPs, whose explicit spatial distribution is not modelled in this work and are, employing a strong assumption, available where needed, are likewise attributed to their closest SS. In the simplest scenario, a census section contains exactly one SS. In such cases, all trip arrivals occurring within the section are assigned to that SS. When multiple substations are found within the same census section, the associated trip arrivals are distributed evenly among them. Conversely, suppose a census section contains no SSs. In that case, all its trip arrivals are rerouted to the nearest census section (identified via Euclidean distance among centroids), after which one

Table 5
Example of permanence matrix.

	00:00	01:00	…	06:00	07:00	08:00	…	21:00	22:00	…	23:00	
Sect. α	20	20	…	20	6	15	…	20	20	…	20	
…				…				…				…
Sect. γ	195	195	…	195	201	358	…	300	195	…	195	

of the two aforementioned allocation rules is applied. This rationale is described in Algorithm 1 and depicted in Fig. 3.

Due to the scope and resolution of the OD matrix, no robust assumption can be made about trip chains (i.e. trips composed of multiple stops), and all recharging processes are thus assumed to be performed at the indicated point of the final destination.

2.3.3. Building the load profile

The evolution of the number of vehicles is translated into a power profile by following some simplifying assumptions about the charging processes, articulated for each of the twelve scenarios. As a notation, subscript pb indicates EVTs that recharge at public infrastructures and pt indicates conversely those recharging at home. The probability ρ, set for each scenario, governs public trip recharging and determines the outcome of the binary variable z_j^{pb}. Moreover, only a fraction of vehicles arriving at their home location is assumed to initiate a charging event. Across all scenarios, the private recharging probability is modelled by variable δ, and directly affects the outcome of x_j^{pt}. This assumption is intended to provide a conservative yet representative scenario, considering the lack of relevant data for this parameter. Furthermore, specific

Algorithm 1 Geographical matching of EVT arrivals to SSs.

Require: Set of census sections C with trip arrivals; set of substations $\mathcal{S}$ with known locations.

```
for each census section c ∈ C do
    S_c = substations located inside c
    if |S_c| = 1 then
        Assign all trip arrivals in c to the unique substation in S_c
    else if |S_c| > 1 then
        Evenly distribute trip arrivals in c among substations in S_c
    else
        Identify nearest census section, c* via Euclidean distance
        S_c* = substations in nearest section
        if |S_c*| = 1 then
            Assign arrivals of c to that substation
        else
            Evenly distribute arrivals of c among substations in S_c*
        end if
    end if
end for
```

characteristics of charging processes, such as peak asynchrony and variability in power demand, are represented through a coincidence factor, cf. For public charging, cf is set to 25%, consistent with [28]. For private charging, cf is instead modelled as a function of the aggregate arrivals at each SS within each time frame. It is computed according to Eq. (6) developed by Bollerslev et al. [45], adopting one of their fit parameters set $[\hat{k}, \hat{\gamma}, \hat{c}]$:

$$cf_\tau^s = \hat{k} \cdot \left(\frac{1}{A_\tau^s}\right)^{\hat{\gamma}} + \hat{c} \tag{6}$$

where A_τ^s is the total number of vehicles *attracted* to the relevant SS s in the time frame τ.

The algorithm cycles through the EVT datasets and accumulates the computed incremental power of each vehicle in the relevant cell of the matrix, with an hourly resolution, to build the power profiles. Eq. (7) summarises the modelling of the power profile in the case of outward trips:

$$P_\tau^{s,pb} = \sum_{j \in A_{pb}} z_j^{pb} \cdot cf_{\tau,s}^{pb} \cdot P_j^{pb} \tag{7}$$

where z_j^{pb} is the binary decision variable for the recharging process of vehicle j, extracted randomly with a ρ probability, typical for each scenario. Eq. (8) reports instead the modelling of the recharging power in the case of private trips:

$$P_\tau^{s,pt} = \sum_{j \in A_{pt}} x_j^{pt} \cdot cf_{\tau,s}^{pt} \cdot P_j^{pt} \tag{8}$$

where x_j^{pt} is the binary decision variable for the recharging process of vehicle j. τ indicates the time frame, cf is the coincidence factor and P_j^{pt} is the nominal power of the CP, randomly extracted from the scenarios presented in Table 8.

Lastly, the overall incremental profile for a given SS s and time frame τ is obtained by summing the two contributions:

$$P_\tau^s = P_\tau^{s,pb} + P_\tau^{s,pt} \tag{9}$$

Each EVT recharging process is subjected to an MC procedure to extract the average incremental charging profile over the relevant time intervals. This approach is adopted to account for the variability of the

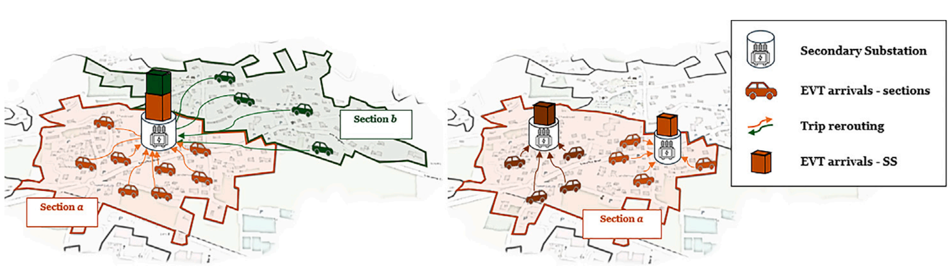

Fig. 3. Geographical matching procedure. On the left, the case with no SS in *Section b*. On the right, the case with multiple SS in a single *section*.

installed charging point portfolio, thereby providing a statistically more stable representation of the average charging behaviour of individual EVTs. Given that a single parameter is subject to stochastic variation, an empirical number of 1000 iterations is selected.

A more informative parameter calibration procedure, grounded in real data from the case study area, could not be performed, as the available data do not suffice to robustly support such an approach. Furthermore, to the authors' knowledge, no empirical information on domestic recharging processes is currently available.

These hourly profiles are accumulated in the recharging demand, which is modelled as an MV load connected to the relevant SS. Since no reactive power exchange is simulated, the loads are operated with a unitary power factor.

2.3.4. Qualitative assessment

The outcome of this procedure provides valuable results even in circumstances in which a comprehensive digital twin of the DN is not available. The enriched GIS layers can, in fact, support wide and systematic investigations into e-mobility patterns and potential energy demand for recharging. These analyses, here defined as qualitative as they do not yet deal with simulations on the DN itself, aim to provide a punctual insight into the most affected grid elements without considering the state of the electrical variables of the grid and its operating conditions. Several metrics to estimate potential criticalities on the network's elements are proposed. One is the Peak-to-Nominal Power Ratio, PNPR, defined in Eq. (10) as the ratio between the daily absorption peak recorded at the SS s, P_s, and the nominal power of the same SS, $P_{nom,s}$:

$$\mathrm{PNPR_s} = \frac{P_s}{P^s_{nom}} \tag{10}$$

Along with this metric, the cumulative vehicle-hour, $\mathrm{veh_s}$, previously introduced, and EV arrivals, A_s^{EV}, at each SS are evaluated.

2.3.5. Quantitative assessment: quasi-dynamic simulation

As anticipated, the availability of a detailed digital twin of the DN allows for bridging the geo-referenced study of mobility to its punctual impact on the corresponding portions of the network. In this study, a detailed assessment of the impact of e-mobility on the grid is obtained by way of a daily load flow (also called QDS) for each scenario. While the comprehensive model of the network is populated with a year's worth of hourly power profiles, the limited scope of the input traffic data, which only tracks one weekday, constrains the analysis to a one-day load flow. To represent the worst-case scenario, a day characterised by high demand is selected as the base scenario.

Unlike the qualitative assessment presented above, which provides an outlook of the load due to mobility trends decoupled from the actual operation of the power system, the comparison of QDSs allows for an estimation of the impact of the incremental load due to EV recharging demand with respect to actual operating conditions. This addresses one critical issue in the integration of new demand, particularly one as time-dependent as e-mobility, which is the synchronicity of loads. The simulation considers one day of operation and integrates the recharging demand as an MV synthetic load connected at every SS, representing the aggregated and composite power profile made up of private and public recharging demand.

To provide an overview of the impact on different elements of the grid, busbar voltages and loading of MV branches and transformers are recorded. DSOs in Italy must operate the network according to operational constraints. Namely, busbar voltages must remain within ±10% of the nominal voltage level. Lines and transformers, on the other hand, are to be operated below the maximum loading of 100%, and the study assumes this as a simplified operating condition.

The outputs stored from the two analyses provide a comprehensive look at the possible evolution of impact on the DN operation.

3. Case study definition and input data

The framework is implemented on a case study in Valle d'Aosta, a mountainous region with 122,000 inhabitants and an extension of approximately 3270 km^2, located in northern Italy, with Aosta as its capital city. Several reasons led to the selection of this case study, based on the ongoing collaboration with the DSO of the Region, Deval [46]. First, the DSO provided a high-resolution digital model of the DN, created using the power system simulation software DIgSILENT PowerFactory. This allows for accurate and precise implementations and the opportunity to test the entire framework. The model represents the network in one standard operating topology and is populated with hourly power profiles for each element down to the SS, which is the finest granularity required. A qualitative assessment of e-mobility impact can be computed with a partial knowledge of the grid; in this case, the minimum requirement is the location and nominal installed power of the SSs.

The opportunity to work on precious and rarely available data clearly elevates the scientific output of the study. Furthermore, this study can be identified within a series of efforts to strengthen the scenario modelling approach, which is crucial to comply with future energy policies [47]. Specifically, this work provides a blueprint for DN planning studies.

Critical demographic information is obtained from periodic census surveys conducted by the National Statistics Agency, ISTAT [39,48]. The data is provided in the form of a GIS-based dataset and numerous thematic tables containing socio-demographic and economic data for each census section in the nation. ISTAT also provides the OD matrix adopted to elaborate on the mobility patterns [41]. This dataset tracks and periodically updates trips representing daily travel patterns on a standard working day and includes information such as origin and destination zones, provinces, departure times, trip purposes, and traveller roles. The transportation network is modelled using the regional road infrastructure, sourced from OpenStreetMaps (OSM) [49] in GIS format.

A critical aspect of this study is defining a mobility scenario to characterise the future degree of light-duty transportation electrification. The scenario is detailed in the Regional Energetic Plan (PEAR) [50], which indicates the target volume of EVs circulating in the territory in 2030. Granular projections at a municipal level are obtained by rescaling the overall volume, leveraging the current shares of EV distribution, updated annually by ACI [51], the Italian public vehicle registry.

As previously introduced in this work, this procedure and case study can be adopted as a comparison with a similar framework. With particular reference to the considerations elaborated in Section 2, and detailed in Tables 2 and 6, it provides an overview of the actual differences in this comparative approach between frameworks.

3.1. Mobility data

The OD matrix adopted is part of a nationwide effort by ISTAT to track the mobility trends of Italian commuters on one typical working day. Records store the purposes of the trip, gender, departure and arrival city and a schedule. The latter is quite poor in detail. The departure time frames are aggregated into only four intervals: i) before 7.15 am; ii) 7.15

Table 6
Comparison of the two study cases.

Travels' features	Existing works [9,18,38]	Present work
Temporal extension	Single sample weekday	Single sample weekday
Study area	Lombardy region	Valle d'Aosta region
OD data publisher	Lombardy Region	ISTAT
Census sections	53k	1.9k
Geographical definition	Calculated - Sub-municipal	Calculated - Sub-municipal
Number of trips	8 million	70k
Projected EVs in 2030	852k	15k
Distribution network	Not available	Available

Table 7
Scenarios compared in this work.

	Considerable CP congestion	No CP congestion
Projected 2030 EV adoption	*Scenario 1* ρ = 50% - 15,000 EVs δ = 25%	*Scenario 2* ρ = 100% - 15,000 EVs δ = 25%
	Scenario 3 ρ = 50% - 15,000 EVs δ = 50%	*Scenario 4* ρ = 100% - 15,000 EVs δ = 50%
	Scenario 5 ρ = 50% - 15,000 EVs δ = 75%	*Scenario 6* ρ = 100% - 15,000 EVs δ = 75%
Halved projected 2030 EV adoption	*Scenario 7* ρ = 50% - 7500 EVs δ = 25%	*Scenario 8* ρ = 100% - 7500 EVs δ = 25%
	Scenario 9 ρ = 50% - 7500 EVs δ = 50%	*Scenario 10* ρ = 100% - 7500 EVs δ = 50%
	Scenario 11 ρ = 50% - 7500 EVs δ = 75%	*Scenario 12* ρ = 100% - 7500 EVs δ = 75%

Table 8
Charging demand scenario.

	Public DC		Public AC	Private AC	
Power [kW]	150	50	22	7.4	3.7
Probability [%]	10	25	65	50	50

- 8.14 am; iii) 8.15 - 9.14 am; and iv) after 9.15 am, as well as the travel times, which are also grouped into four categories: i) up to 15min; ii) 16 - 30min; iii) 31 - 60min; and iv) more than 60min. This lack of temporal detail justifies the efforts detailed in Section 2 to improve the resolution.

3.2. Demand scenarios

This study adopts the scenarios summarised in Table 7, which are differentiated by the volume of circulating EVs, the availability of CPs and the share of EV users domestically recharging their vehicles. Additionally, a real-life 2022 operating base scenario is also evaluated. As this work does not model the recharging infrastructure, a statistical parameter ρ is adopted to simulate its availability, modelling the probability of an EV driver finding an available CP upon arrival at the destination. δ governs instead the share of EV drivers recharging their vehicles at home once arrived. *Scenarios 7–12* represent a halved adoption of EVs in the Region, simulating a conservative scenario for policy goals. Parameter ρ is set to model an unconstrained demand scenario, referred to as *No CP congestion*, and a constrained one, simulating a CP rollout not adequate to accommodate the needs of EV drivers choosing public recharge.

Each CP is characterised by a nominal power extracted from the distributions reported in Table 8, modelled based on future projections [52], current rollout in the region and consistent with literature assumptions [28,32].

3.3. Medium voltage distribution network

The investigated distribution network studied is managed by Deval [47]. The High Voltage (HV) network, regulated by the national Transmission System Operator, connects the MV grid to the national grid. Aligning with other Italian distribution systems, typical voltage levels are 132 kV for HV and 15 kV for MV. Due to the specific orography of the region, the MV network features several feeders longer than the Italian average. Furthermore, for geographical, economic and historical reasons, large hydro generators play a significant role in the local energy mix, while MV loads are mostly modest in size. Table 9 provides some information on the extent and characteristics of the regional grid, while Fig. 4 shows an overview of the digital twin of the regional network.

Table 9
Distribution network [47].

Metric	Quantity
HV/MV substations (PS)	14
MV/MV substations	6
MV/LV substations (SS)	1520
Users connected	130,000
MV network extension [km]	1552
MV cable/line ratio	0.86
MV passive users (2024) [MW]	64.6
Energy produced - MV (2024) [MWh]	590,196
LV network extension [km]	2729
LV cable/line ratio	1.05
LV passive users (2024) [MW]	540.5
Energy produced - LV (2024) [MWh]	33,434

4. Results and discussion

4.1. Qualitative impact assessment

The traffic procedure is run for the entire Region and returns a detailed overview of EVT flows at a geographical and electrical layer. The region-wide outcome of the traffic and EV selection procedures is reported in Fig. 5, which provides an overview of arrivals at census sections and is mapped onto the SSs in the entire region. Despite the wide scope captured by the picture, it is straightforward to identify a hotspot for EV traffic in the region. This visual result is corroborated by the statistical outline of the qualitative assessment reported in Table 10. A comparison of median values and percentile analysis underlines the concentration of e-mobility towards the tail of the distribution of SSs, particularly in a restricted subset of grid elements located in the largest urban settlement in the region, which is the city of Aosta (its administrative borders are reported in Fig. 5). In the following section, the quantitative assessment further substantiates this evidence.

4.2. Quantitative impact assessment

To represent a heterogeneous yet significant set of SSs, comprising a mix of mostly industrial, commercial and residential configurations, five exemplary power profiles for *Scenario 6*, obtained with the procedure detailed in Section 2, are presented in Fig. 6. The temporal distribution of the power profiles throughout the day can provide indications regarding the functional characteristics and likely location of the SSs. For instance, profiles exhibiting pronounced peaks during the central hours are likely to be associated with areas predominantly subject to work-related trips (e.g. *'SS 5'* and *'SS 1'* pictured). Conversely, profiles with significant activity during off-peak hours are generally indicative of residential or private charging patterns (e.g. *'SS 4'* pictured).

Table 11 reports the comprehensive quantitative results for the scenarios studied, evaluated by the metrics introduced. The percentile distributions are computed on the peak power value for each grid element across the day, and the thresholds reported are chosen to depict the significant, although marginal, impact on the grid. The majority of the network remains well within standard operating conditions, highlighting the adequacy of the grid in place. The Cumulative Distribution Function (CDF) of the same data, limited to bus voltages and branch loadings of *base scenario* and *Scenario 6*, is reported in Fig. 7.

As the percentile distributions show, the impact of EVTs is quite limited for the majority of the network, as critical values are only reached

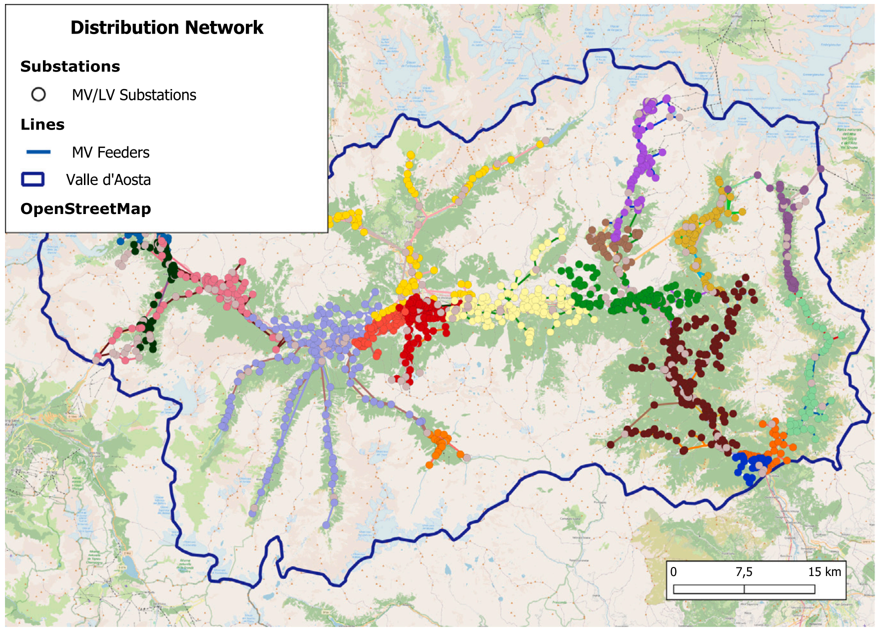

Fig. 4. Regional distribution network.

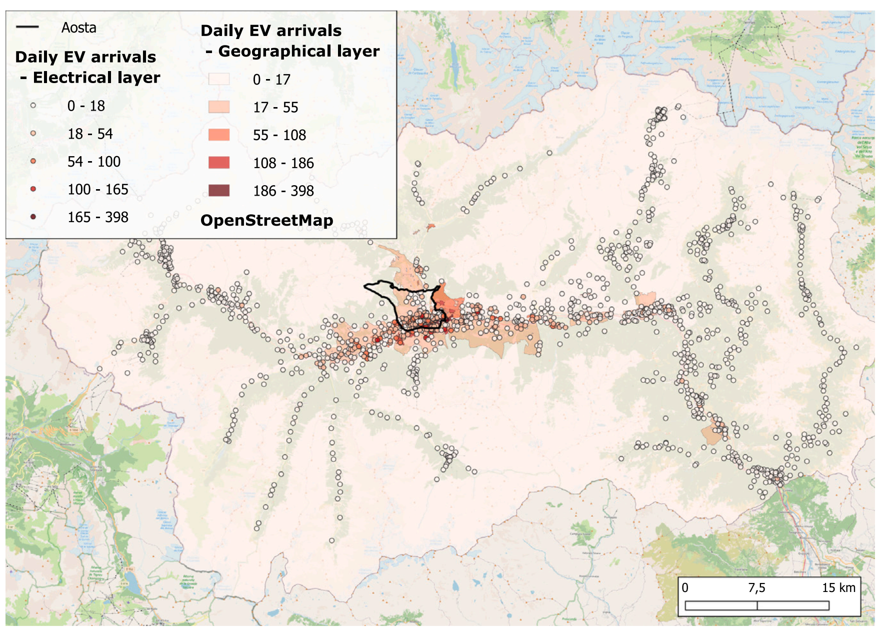

Fig. 5. Distribution of EV arrivals in census sections and SSs.

in the top percentiles and thus affect only a portion of the network. The comparison of voltage levels across the grid is reported in Fig. 8 with boxplots representing an overview of MV busbar voltage distribution across the scenarios. In scenarios with $\rho = 100\%$, where all EVs request a public recharge, some busbars reach voltages as low as 0.97 p.u. Since no generation is added to the base scenario, no voltage rise is observed. This suggests that, under the assumed mobility trends and charging infrastructure hypotheses, the impact of public recharging on the network far outweighs that of residential recharging, which involves lower individual power levels. The 10 most impacted busbars, recognised as those reporting the greatest voltage drop compared to the *base scenario*, are selected for representation in Fig. 9, where a three-dimensional plot depicts the voltage evolution throughout the simulated day. Fig. 10 shows a heatmap of the voltage levels, centered around the city of Aosta, elaborated using the same results, sampled at 11 am.

The increased load causes significant stress on the feeders and transformers, as the maximum values of loading computed across case studies are nearly doubled. Fig. 11 reports the comparison of loadings for MV branches across five scenarios. On the other hand, voltages remain within expected thresholds.

Table 10
Qualitative results (98th–100th percentiles, median in parentheses).

	PNPR [p.u.]	Peak power [kW]	veh [k(vehicle·h)]	EV arrivals
Scenario 1	1.5 – 9.9 (0.06)	363.5 – 3846 (10.0)	5.2 – 18.5 (0.14)	77 – 398 (2)
Scenario 2	3.0 – 19.8 (0.10)	721.8 – 7690 (19.8)		
Scenario 3	1.5 – 9.9 (0.07)	361.8 – 3839 (10.2)		
Scenario 4	3.0 – 19.9 (0.12)	722.3 – 7698 (19.9)		
Scenario 5	1.5 – 9.9 (0.08)	360.1 – 3857 (12.3)		
Scenario 6	3.0 – 19.9 (0.13)	722.5 – 7689 (19.9)		
Scenario 7	1.3 – 8.5 (0.03)	327.6 – 3403 (5.5)	3.5 – 16.1 (0.07)	54 – 347 (1)
Scenario 8	2.6 – 17.1 (0.06)	657.3 – 6834 (10.0)		
Scenario 9	1.3 – 8.6 (0.04)	328.5 – 3421 (6.6)		
Scenario 10	2.6 – 17.1 (0.07)	657.0 – 6838 (11.3)		
Scenario 11	1.3 – 8.5 (0.04)	327.1 – 3404 (7.6)		
Scenario 12	2.6 – 17.1 (0.07)	655.2 – 6833 (12.4)		

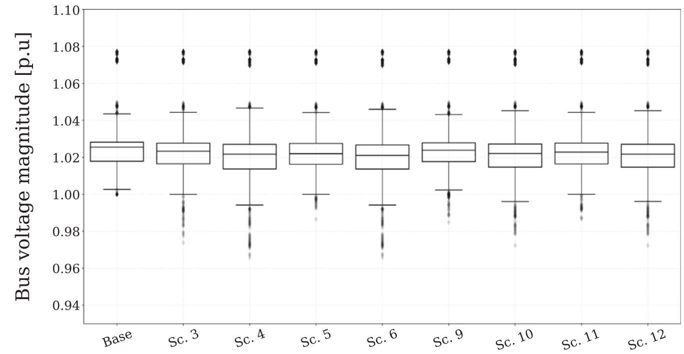

Fig. 8. Boxplot of busbar voltages in each scenario.

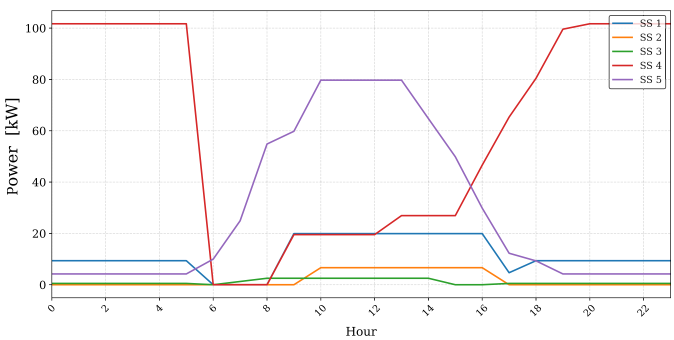

Fig. 6. Hourly power profile of a representative set of five SSs.

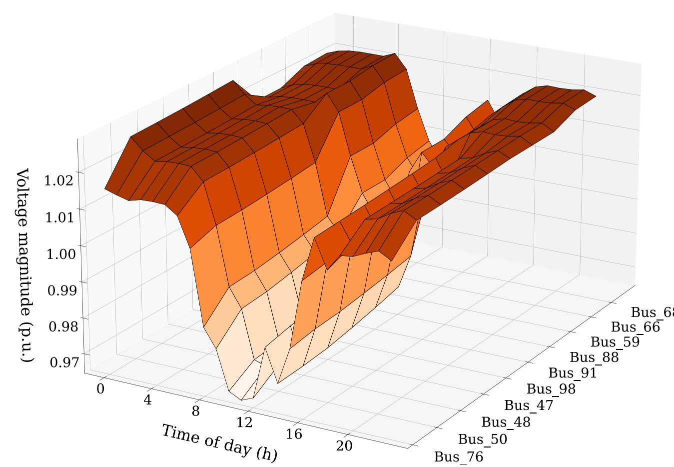

Fig. 9. Daily voltage in the most impacted busbars (georeferenced in Fig. 12).

Table 11
QDS results (98–100 percentiles for loadings, 0–2 for voltages). The percentile within parentheses indicates the operational limit violation.

Scenario / Metric	Branch loading [%]	Trafo loading [%]	Bus voltage [p.u.]
Base	44.7 – 112.8 (99.9)	30.3 – 67.6 (-)	1.00 – 1.02 (-)
Scenario 1	50.7 – 112.8 (99.9)	30.3 – 96.1 (-)	0.99 – 1.01 (-)
Scenario 2	67.0 – 159.2 (99.9)	30.5 – 175.8 (99.9)	0.97 – 1.00 (-)
Scenario 3	50.2 – 112.8 (99.9)	30.3 – 96.1 (-)	0.99 – 1.01 (-)
Scenario 4	66.9 – 159.3 (99.9)	30.5 – 176.0 (99.9)	0.97 – 1.00 (-)
Scenario 5	50.2 – 112.8 (99.9)	30.3 – 96.1 (-)	0.99 – 1.01 (-)
Scenario 6	67.0 – 159.4 (99.9)	30.6 – 176.0 (99.9)	0.97 – 1.00 (-)
Scenario 7	50.2 – 112.8 (99.9)	30.3 – 84.6 (-)	0.99 – 1.01 (-)
Scenario 8	59.3 – 137.9 (99.9)	30.3 – 151.5 (99.9)	0.97 – 1.00 (-)
Scenario 9	50.0 – 112.8 (99.9)	30.3 – 84.7 (-)	0.99 – 1.01 (-)
Scenario 10	59.3 – 137.9 (99.9)	30.4 – 151.5 (99.9)	0.97 – 1.01 (-)
Scenario 11	50.0 – 112.8 (99.9)	30.3 – 84.6 (-)	0.99 – 1.01 (-)
Scenario 12	59.4 – 138.0 (99.9)	30.4 – 151.6 (99.9)	0.97 – 1.00 (-)

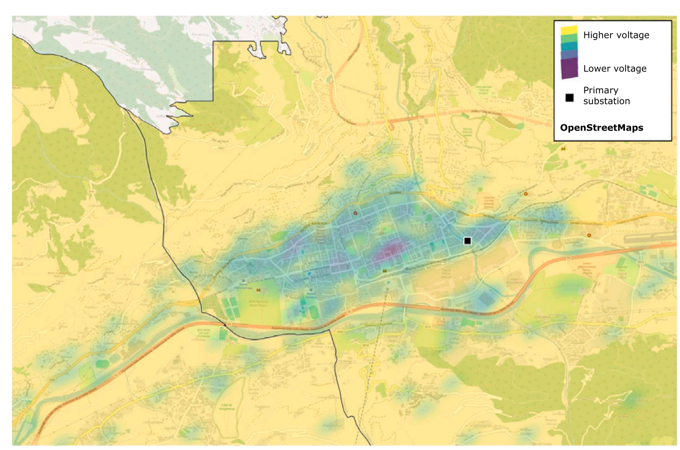

Fig. 10. Heatmap of voltages during the peak timeframe, around the city of Aosta.

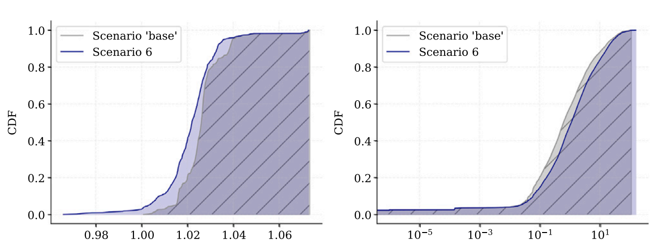

Fig. 7. CDF for *Base Scenario* and *Scenario 6*.

The combination of qualitative and quantitative results provides a focused outlook for the territory surrounding the city of Aosta, shown in Fig. 12. EV arrivals in the census sections are mapped along the EVTs distributed onto the SSs. Additionally, the most affected busbars (pictured in Fig. 9) are also mapped. Nine out of the ten busbars lie within the restricted portion of the region highlighted in the figure.

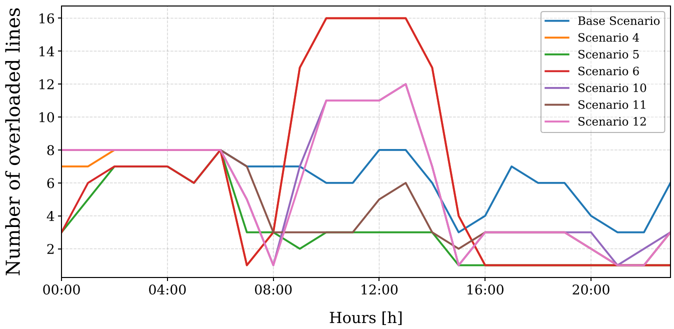

Fig. 11. Number of overloaded lines during the simulated day across the scenarios.

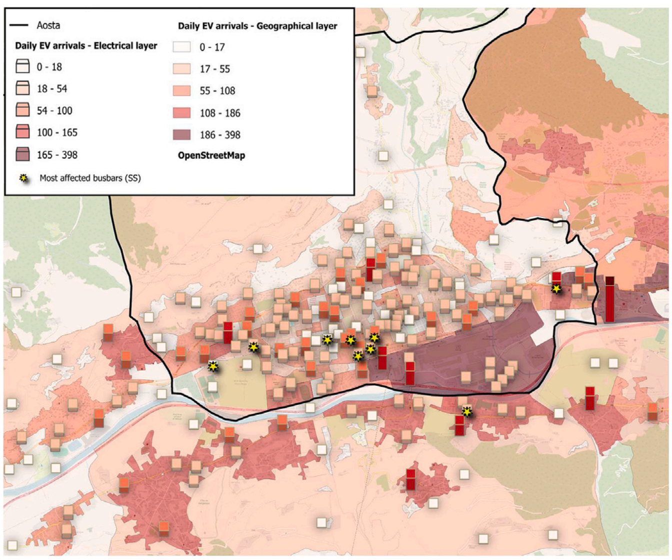

Fig. 12. Geo-referenced overview of the EV arrivals (focused on the city of Aosta).

5. Conclusions

This study adopts a detailed mobility model to simulate the traffic flow of EVs in Valle d'Aosta on a typical workday, enriching the analysis with an ML EV selection routine based on trip features and socio-economic characteristics of drivers. The framework is geo-referenced and allows for precise identification of the recharging demands on the electrical network. The e-mobility results obtained inform the calculation of load profiles that represent private and public recharging processes based on mobility patterns in twelve different scenarios simulating congested (constrained) and uncongested demand. The profiles are then modelled as synthetic MV loads connected to each SS in the network, which are integrated in the DigSILENT digital twin of a real Regional MV DN.

The presented outputs yield two analyses. A qualitative geo-referenced evaluation of mobility impacts can be performed without the grid model. Conversely, a daily load flow provides an accurate quantitative and tangible understanding of the operational condition of the network under the simulated scenarios. Both analyses demonstrate that the existing grid infrastructure is largely capable of accommodating EV adoption targets set for 2030.

The main limitations of the proposed framework stem from the restricted temporal scope of the underlying traffic data. As shown in Table 6, the OD matrices capture trips for a single representative weekday. This constraint becomes especially problematic when the goal is to obtain a yearly perspective capable of capturing seasonality and other non-recurring effects. In this work, for instance, the yearly power profiles available for the whole grid could not be leveraged, owing to the absence of compatible yearly e-mobility profiles. Furthermore, the traffic described by the input matrices is closely tied to commuting and study-related trips, and, crucially, no other compatible publication is available to complement this dataset with the information needed to model mobility patterns for different days or scenarios. As a result, the findings are only representative of the single weekday captured by the survey, and extending the analysis to other days would require repeating the entire procedure on separate datasets. Finally, investigations focused on specific areas, such as tourism hotspots, would benefit from an explicit model of tourist traffic, which introduces additional complexity in terms of both the volume and the pattern of circulating vehicles.

Additionally, better calibration of key steps in the procedure could be achieved as e-mobility trends and recharging data become more widely available in the coming years. In this regard, the future deployment of observability on domestic recharging devices within the Italian regulatory framework could provide ample opportunities for more precise studies.

This paper expands on the procedure presented in previous works, proposing a methodology to achieve an estimation of e-mobility in the case of severely sparse traffic data. Furthermore, the framework is enriched with the implementation of a two-level impact estimation on the digital network of a large MV DN. The findings offer effective insights for DSOs, supporting more targeted and informed planning strategies to identify and prioritise areas most at risk of network stress.

CRediT authorship contribution statement

Davide Fratelli: Writing – review & editing, Writing – original draft, Visualization, Validation, Software, Methodology, Investigation, Data curation, Conceptualization. **Corrado Maria Caminiti:** Writing – review & editing, Writing – original draft, Validation, Methodology, Investigation, Formal analysis, Conceptualization. **Matteo Spiller:** Writing – review & editing, Validation, Software, Data curation, Conceptualization. **Aleksandar Dimovski:** Writing – review & editing, Supervision, Methodology, Conceptualization. **Marco Merlo:** Writing – review & editing, Supervision, Project administration, Methodology, Conceptualization.

Declaration of competing interest

The authors declare that they have no known competing financial interests or personal relationships that could have appeared to influence the work reported in this paper.

Acknowledgements

The authors would like to thank Deval S.p.A. for the data kindly provided. Deval S.p.A. also funds Davide Fratelli's scholarship (40th PhD call - PNRR 630). Corrado Maria Caminiti's scholarship is funded by ABB S.p.A. (Italy).

Data availability

The data that has been used is confidential.

References

[1] W. Johnny, What does net zero emissions mean and how can we get there? 2021, https://www.weforum.org/stories/2021/11/net-zero-emissions-cop26-climate-change/ (Accessed on 4 November 2025).

[2] S. Alexander, An overview of Federal government support for electric vehicles, 2023, https://www.instituteforenergyresearch.org/regulation/an-overview-of-federal-government-support-for-electric-vehicles/ (Accessed on 4 November 2025).

[3] ACEA, Fiscal support to stimulate market uptake of electric cars in European countries, 2024, https://www.acea.auto/fact/electric-cars-tax-benefits-and-incentives-2024/ (Accessed on 4 November 2025).
[4] European Commission, Fit for 55 - consilium, 2024, https://www.consilium.europa.eu/policies/fit-for-55/ (Accessed on 11 November 2024).
[5] IEA, World energy outlook 2025, 2025, https://www.iea.org/reports/world-energy-outlook-2025 (Accessed on 4 November 2025).
[6] IEA, Global EV outlook 2023. Catching up with climate ambition, 2023, https://www.iea.org/reports/global-ev-outlook-2022 (Accessed on 28 March 2023).
[7] A. Mohammed, O. Saif, M. Abo-Adma, A. Fahmy, R. Elazab, Strategies and sustainability in fast charging station deployment for electric vehicles, Sci. Rep. 14 (1) (2024) 283, https://doi.org/10.1038/s41598-023-50825-7
[8] Y. Mu, J. Wu, N. Jenkins, H. Jia, C. Wang, A spatial–temporal model for grid impact analysis of plug-in electric vehicles, Appl. Energy 114 (2014) 456–465, https://doi.org/10.1016/j.apenergy.2013.10.006
[9] C.M. Caminiti, L.G. Brigatti, M. Spiller, G. Rancilio, M. Merlo, Unlocking grid flexibility: leveraging mobility patterns for electric vehicle integration in ancillary services, World Electr. Veh. J. 15 (9) (2024), https://doi.org/10.3390/wevj15090413
[10] Z. Yi, B. Chen, X.C. Liu, R. Wei, J. Chen, Z. Chen, An Agent-Based Modeling Approach for Public Charging Demand Estimation and Charging Station Location Optimization at Urban Scale, Computers, Environment and Urban Systems, 2023, https://doi.org/10.1016/j.compenvurbsys.2023.101949, (101) 101949.
[11] T. Novosel, L. Perković, M. Ban, H. Keko, T. Pukšec, G. Krajačić, N. Duić, Agent based modelling and energy planning – utilization of MATSim for transport energy demand modelling, Energy 92 (2015), https://doi.org/10.1016/j.energy.2015.05.091
[12] K.W. Axhausen, A. Horni, K. Nagel, The Multi-Agent Transport Simulation MATSim, Ubiquity Press / OAPEN, 2016, Open-Access book, OAPEN Library.
[13] Y. Mu, J. Wu, N. Jenkins, H. Jia, C. Wang, A spatial–temporal model for grid impact analysis of plug-in electric vehicles, Appl. Energy 114 (2014) 456–465, https://doi.org/10.1016/j.apenergy.2013.10.006
[14] Q. Yang, R. Balakrishna, D. Morgan, H. Slavin, Large-scale, high-fedelity dynamic traffic assignment: framework and real-world case studies, Transp. Res. Procedia 25 (2017) 1290–1299, World Conference on Transport Research - WCTR 2016 Shanghai. 10–15 July 2016. https://doi.org/10.1016/j.trpro.2017.05.152
[15] Y. Kudoh, H. Ishitani, R. Matsuhashi, Y. Yoshida, K. Morita, S. Katsuki, O. Kobayashi, Environmental evaluation of introducing electric vehicles using a dynamic traffic-flow model, Appl. Energy 69 (2) (2001) 145–159, https://doi.org/10.1016/S0306-2619(01)00005-8
[16] F.J. Soares, J.A. Peças Lopes, P.M. Rocha Almeida, A Monte Carlo method to evaluate electric vehicles impacts in distribution networks, in: 2010 IEEE Conference on Innovative Technologies for an Efficient and Reliable Electricity Supply, 2010, pp. 365–372, https://doi.org/10.1109/CITRES.2010.5619777
[17] H. Li, H. Qu, X. Tan, L. You, R. Zhu, W. Fan, UrbanEV: an open benchmark dataset for urban electric vehicle charging demand prediction, Sci. Data 12 (1) (2025) 523, https://doi.org/10.1038/s41597-025-04874-4
[18] G. Yousefi, A. Dimovski, L. Radaelli, M. Merlo, Estimating the impact of electric mobility on distribution networks through GIS techniques, Sustain. Energy Grids Netw. 38 (2024), https://doi.org/10.1016/j.segan.2024.101379
[19] C. Rong, J. Ding, Y. Liu, Y. Li, A large-scale benchmark dataset for commuting origin-destination matrix generation, Accessed on arXiv:2407.15823, 2024 (4 November 2025).
[20] J.H.M. Langbroek, J.P. Franklin, Y.O. Susilo, Electric vehicle users and their travel patterns in greater Stockholm, Transp. Res. D Transp. Environ. 52 (2017) 98–111, https://doi.org/10.1016/j.trd.2017.02.015
[21] R. Danielis, L. Rotaris, M. Giansoldati, M. Scorrano, Drivers' preferences for electric cars in Italy. Evidence from a country with limited but growing electric car uptake, Transp. Res. A Policy Pract. 137 (2020) 79–94, https://doi.org/10.1016/j.tra.2020.04.004
[22] J. Jia, B. Shi, F. Che, H. Zhang, Predicting the regional adoption of electric vehicle (EV) with comprehensive models, IEEE Access 8 (2020) 147275–147285, https://doi.org/10.1109/ACCESS.2020.3014851
[23] F.H.A. (2022), 2022 NextGen national household travel survey core data, U.S. department of transportation, Washington, DC, Available online: 2022, http://nhts.ornl.gov (Accessed on 4 November 2025).
[24] R.J. Javid, A. Nejat, A comprehensive model of regional electric vehicle adoption and penetration, Transp. Policy 54 (2017) 30–42, https://doi.org/10.1016/j.tranpol.2016.11.003
[25] F. Miconi, G.M. Dimitri, A machine learning approach to analyse and predict the electric cars scenario: the Italian case, PLoS One 18 (1) (2023) e0279040, https://doi.org/10.1371/journal.pone.0279040
[26] W. Li, R. Long, H. Chen, J. Geng, A review of factors influencing consumer intentions to adopt battery electric vehicles, Renew. Sustain. Energy Rev. 78 (2017) 318–328, https://doi.org/10.1016/j.rser.2017.04.076
[27] ETIP SNET Working Group 1, E-mobility Deployment and Impact on Grids: Impact of EV and Charging Infrastructure on European T&D Grids – Innovation Needs, ISBN 978-92-76-53455-6; Catalogue number MJ-09-22-246-EN-N; (2022, https://doi.org/10.2833/937755 (Accessed on 4 November 2025).
[28] P. Eitel, P. Stolle, A machine learning approach to model the future distribution of e-mobility and its impact on the power grid, Energy Inform. 5 (1) (2022) 31, https://doi.org/10.1186/s42162-022-00203-w
[29] E. Veldman, M. Gibescu, H.J.G. Slootweg, W.L. Kling, Scenario-based modelling of future residential electricity demands and assessing their impact on distribution grids, Energy Policy 56 (2013) 233–247, https://doi.org/10.1016/j.enpol.2012.12.078
[30] E. Veldman, R.A. Verzijlbergh, Distribution grid impacts of smart electric vehicle charging from different perspectives, IEEE Trans. Smart Grid 6 (1) (2015) 333–342, https://doi.org/10.1109/TSG.2014.2355494
[31] F. Salah, J.P. Ilg, C.M. Flath, H. Basse, C.V. Dinther, Impact of electric vehicles on distribution substations: a Swiss case study, Appl. Energy 137 (2015) 88–96, https://doi.org/10.1016/j.apenergy.2014.09.091
[32] R. Gupta, A. Pena-Bello, K.N. Streicher, C. Roduner, Y. Farhat, D. Thöni, M.K. Patel, D. Parra, Spatial analysis of distribution grid capacity and costs to enable massive deployment of PV, electric mobility and electric heating, Appl. Energy 287 (2021), https://doi.org/10.1016/j.apenergy.2021.116504
[33] J. Vopava, C. Koczwara, A. Traupmann, T. Kienberger, Investigating the impact of E-Mobility on the electrical power grid using a simplified grid modelling approach, Energies 13 (11) (2020) 39, https://doi.org/10.3390/en13010039
[34] S.M. Arif, T.T. Lie, B.C. Seet, S.M. Ahsan, H.A. Khan, Plug-in electric bus depot charging with PV and ESS and their impact on LV feeder, Energies 13 (9) (2020), https://doi.org/10.3390/en13092139
[35] V. Subramanian, F. Feijoo, S. Sankaranarayanan, K. Melendez, T.K. Das, A bilevel conic optimization model for routing and charging of EV fleets serving long distance delivery networks, Energy 251 (2022) 123808, https://doi.org/10.1016/j.energy.2022.123808
[36] T. Yi, C. Zhang, T. Lin, J. Liu, Research on the spatial-temporal distribution of electric vehicle charging load demand: a case study in China, J. Clean. Prod. 242 (2020) 118457, https://doi.org/10.1016/j.jclepro.2019.118457
[37] Y. Xiang, Z. Jiang, C. Gu, F. Teng, X. Wei, Y. Wang, Electric vehicle charging in smart grid: a spatial-temporal simulation method, Energy 189 (2019) 116221, https://doi.org/10.1016/j.energy.2019.116221
[38] C.M. Caminiti, D. Fratelli, M. Spiller, A. Dimovski, M. Merlo, Integrating bottom-up GIS and machine learning models for spatial-temporal analysis of electric mobility impact on power system, Smart Energy 19 (2025) 100185, https://doi.org/10.1016/j.segy.2025.100185
[39] ISTAT, Dati per sezioni DI censimento, 2023, https://www.istat.it/notizia/dati-per-sezioni-di-censimento/ (Accessed on 23 August 2024).
[40] Matrice OD2016 - passeggeri - scenario 2020 | open data regione lombardia, 2021, https://www.dati.lombardia.it/Mobilit-e-trasporti/Matrice-OD2016-Passeggeri-Scenario-2020/hyqr-mpe2/about_data (Accessed on 4 May 2026).
[41] ISTAT, Matrici del pendolarismo, 2014, https://www.istat.it/non-categorizzato/matrici-del-pendolarismo/ (Accessed on 10 October 2024).
[42] Netherlands Mobility Panel, MPN data, 2022, https://www.mpndata.nl/ (Accessed on 10 June 2024).
[43] S. Hoogendoorn-Lanser, N.T.W. Schaap, M.-J. OldeKalter, The Netherlands mobility panel: an innovative design approach for web-based longitudinal travel data collection, Transp. Res. Procedia 11 (2015) 311–329, https://doi.org/10.1016/j.trpro.2015.12.027
[44] L. Jia, Z. Hu, Y. Song, Z. Luo, Optimal siting and sizing of electric vehicle charging stations, in: 2012 IEEE International Electric Vehicle Conference, 2012, pp. 1–6, https://doi.org/10.1109/IEVC.2012.6183283
[45] J. Bollerslev, P.B. Andersen, T.V. Jensen, M. Marinelli, A. Thingvad, L. Calearo, T. Weckesser, Coincidence factors for domestic EV charging from driving and plug-in behavior, IEEE Trans. Transp. Electrif. 8 (1) (2022) 808–819, https://doi.org/10.1109/TTE.2021.3088275
[46] Deval, Deval spa, 2025, https://www.devalspa.it/ (Accessed on 4 November 2025).
[47] Piano per lo sviluppo delle reti DI distribuzione dell'energia elettrica 2025-2029, 2025, https://www.devalspa.it/piano-di-sviluppo (Accessed on 26 November 2025).
[48] ISTAT, Basi territoriali e variabili censuarie, 2024, https://www.istat.it/notizia/basi-territoriali-e-variabili-censuarie/ (Accessed on 23 August 2024).
[49] OpenStreetMap contributors, Planet dump retrieved from, 2017. https://planet.osm.org., https://www.openstreetmap.org., Accessed on November 04, 2025.
[50] Regione Autonoma Valle d'Aosta, Pianificazione energetica regionale, 2025, https://www.regione.vda.it/energia/pianificazione_energetica_regionale (Accessed on 4 November 2025).
[51] Automobile Club d'Italia, ACI - parco veicoli, 2024, https://www.aci.it/ (Accessed on 15 July 2024).
[52] Motus-E, Il futuro della mobilità elettrica in italia @2035, 2023, https://www.motus-e.org/studi_e_ricerche/il-futuro-della-mobilita-elettrica-in-italia-2035/ (Accessed on 4 November 2025).